

Article

Intermetallic Compounds Formation during 316L Stainless Steel Reaction with Al-Zn-Si Coating Alloy

Abdul Khaliq^{1,2,*}, Abdulaziz S. Alghamdi¹, Mohamed Ramadan^{1,3}, Tayyab Subhani¹, Wajdi Rajhi^{1,4}, Waseem Haider⁵ and Mohammad Mehedi Hasan⁶

¹ College of Engineering, University of Ha'il, P.O. Box 2440, Hail 53962, Saudi Arabia; a.alghamdi@uoh.edu.sa (A.S.A.); m.ramadan@uoh.edu.sa (M.R.); ta.subhani@uoh.edu.sa (T.S.); wajdirajhi@gmail.com (W.R.)

² School of Engineering, RMIT University, Melbourne 3000, Australia

³ Central Metallurgical Research and Development Institute (CMRDI), Helwan 11421, Egypt

⁴ Laboratoire de Mécanique, Matériaux et Procédés LR99ES05, Ecole Nationale Supérieure d'Ingénieurs de Tunis, 5 Avenue Taha Hussein, Montfleury, Université de Tunis, Tunis 1008, Tunisia

⁵ School of Engineering and Technology, Central Michigan University, Mount Pleasant, MI 48859, USA; haide1w@cmich.edu

⁶ Department of Mechanical Engineering and Product Design Engineering, Swinburne University of Technology, Melbourne 3122, Australia; mohammadhasan@swin.edu.au

* Correspondence: ab.ismail@uoh.edu.sa; Tel.: +966-55-6873356

Abstract: Steel products are coated with Aluminum (Al) and Zinc (Zn) alloys to improve their corrosion properties. Bulk steel products are coated in batches; however, steel sheets are coated by a continuous hot-dip galvanizing process. Steel sheets are guided into and out of the molten Al-Zn-Si (AZ) bath with the help of stainless-steel rolls, known as guiding, and sink rolls. These rolls are subjected to excessive surface corrosion with molten AZ bath and, hence, are replaced frequently. The surface deterioration of the immersed rolls has been a long-standing issue in the galvanizing industry. In this study, 316L stainless-steel (SS) rods are immersed in the AZ alloy at 600 °C. The immersion time varied from 1 day to 7 days under the static melt conditions in the iron (Fe)-saturated AZ bath. Microstructural analysis of the immersed SS samples revealed two distinct intermetallic compound (IMC) layers forming between the SS substrate and AZ alloy. The IMC layer 1 (AL-1) formed between the SS substrate and IMC layer 2 (AL-2), growing in thickness from 68 μm to 120 μm within 5 days of immersion. The AL-2, which formed between AL-1 and AZ alloy after 24 h of immersion, then grew in thickness up to 150 μm with an uneven trend. The AL-1 is composed of Fe₂Al₅ and that of AL-2 is composed of FeAl₃ that were predicted by the FactSage thermodynamic analysis. Crack development between AL-1 and AL-2 layers, and disintegration of AL-2 into the AZ bath, are key findings of this study. A drastic hardness increase was observed because the IMC layers produce a hard and brittle sink roll surface.

Keywords: IMCs; Al-Zn-Si alloy; stainless steel; sink rolls; galvanizing; coating



Citation: Khaliq, A.; Alghamdi, A.S.; Ramadan, M.; Subhani, T.; Rajhi, W.; Haider, W.; Hasan, M.M. Intermetallic Compounds Formation during 316L Stainless Steel Reaction with Al-Zn-Si Coating Alloy. *Crystals* **2022**, *12*, 735. <https://doi.org/10.3390/cryst12050735>

Academic Editors: Xiaochun Li and Dejun Li

Received: 11 April 2022

Accepted: 18 May 2022

Published: 20 May 2022

Publisher's Note: MDPI stays neutral with regard to jurisdictional claims in published maps and institutional affiliations.



Copyright: © 2022 by the authors. Licensee MDPI, Basel, Switzerland. This article is an open access article distributed under the terms and conditions of the Creative Commons Attribution (CC BY) license (<https://creativecommons.org/licenses/by/4.0/>).

1. Introduction

Steel products are coated with Zinc (Zn) and aluminum (Al) alloys for their protection against corrosion and other severe environmental conditions. Since the invention of the galvanizing process over 200 years ago, steel has been coated with pure Zn and Zn alloys. Such coating processes are classified as barrier processes. Service steel is isolated from the corrosive environment and the coating alloy is scarified or corroded prior to the steel degradation. For automotive and construction industry applications, Zn-based coatings are alloyed with Al, Si and Mg to achieve better corrosion properties [1]. Commercially, Zn + < 0.3% Al alloy is recognized as Galvanized, Zn + 5% Al as Galfan, Zn + 55% Al + 1.6% Si as Galvalume (AZ) and Zn + 55% Al + 1.6% Si + 2% Mg as Galvalume (AM) [1–3]. Steel is coated with Zn and Al

alloys by hot-dip galvanizing, thermal spraying and electrodeposition routes. However, hot-dip galvanizing is the most versatile process and, hence, has been adopted commercially. Batch and continuous hot-dip galvanizing are the common routes for the coating of industrial steel products. Generally, thick steel products are coated by batch routes and steel sheets or coils are coated by continuous hot-dip galvanizing routes [1,4]. A schematic diagram of a continuous hot-dip galvanizing process is shown in Figure 1.

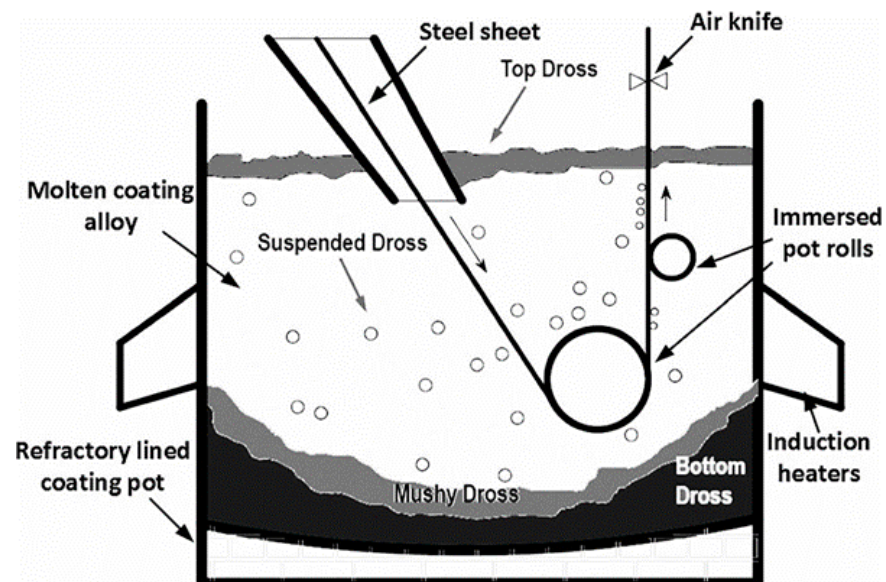


Figure 1. A schematic presentation of continuous hot-dip galvanizing process [2].

In a commercial continuous hot-dip galvanizing process involving AZ or AM coating alloys, a clean and highly activated surface steel strip is immersed into a pot containing alloy melt. The pot temperature ranges from 595 to 610 °C, depending upon the alloy chemistry and type of the steel strip. The pot temperature is maintained with the support of induction heaters, which continuously circulate alloy melt and also supply induction stirring. The pot temperature is maintained precisely by the in-situ thermocouples. However, a temperature fluctuation of ± 1.5 °C is unavoidable due to heat losses during the coating process. A temperature perturbation of ± 10 °C has also been reported in the literature [5,6]. After passing through the alloy melt, the steel strip is coated. The thickness of the coating is maintained by a pair of air knives, which removes extra metal from the surface. A coated steel strip is composed of the following regions: 1. steel substrate, 2. coating alloy or the overlay, and 3. interfacial intermetallic layer between the steel substrate and the overlay. In the AZ coating process, the main framework of the overlay is composed of about 80% α -Al phase containing Zn, and 20% β -Zn in the interdendritic regions. The interfacial intermetallic layer is composed of Fe-Al (FeAl_3 , Fe_2Al_5) and Fe-Al-Si ($\text{Fe}_5\text{Al}_{20}\text{Si}_2$), with 5–7% Zn known as τ_{5c} that has been reported by a previous researcher [7,8]. Iron (Fe) dissolution from the steel strip and formation of Fe-based intermetallic compounds (IMCs) have been reported in the literature [8,9]. Aluminum is highly reactive to steel, hence, forming Fe-based IMCs during the hot-dip galvanizing processes. Such IMCs are undesirable as they are a source of the bottom dross build-up in the coating pot and also a source of metal spot defects in the coated steel products [10,11].

During a continuous hot-dip galvanizing process, a steel strip is guided in and out of the pot with the help of rolls, known as the guiding and stabilizing rolls. In addition to that, sink roll is used to immerse the steel strip, as shown in Figure 1. These rolls and other pot hardware (snout, bolt fixtures and bearings), which continuously remain in contact with the molten alloy, are exposed to excessive corrosion. Considering significantly higher reactivity of Al with Fe, plain carbon steel is not suitable for the fabrication of immersed pot hardware (rolls, snout and bearings) [12–15]. Following are the long-standing issues

of the galvanizing industry: 1. line stoppage due to excessive bottom dross build in the coating pot, 2. steel strip defects due to the suspended IMCs particles, which become part of the overlay, 3. sink, guiding and stabilizing rolls and bearings failure, 4. loss in surface and mechanical properties of the pot gears materials, 5. IMCs particles build up on the rolls surface. These challenges are the main cause of the continuous hot-dip coating lines downtime that result in a significant economic loss to the galvanizing industry. Therefore, selection of the right materials for the pot gears and their corrosion in the coating alloy have been recognized as one of the key factors in resolving the challenges faced by the galvanizing industry [16,17]. Industrially, stainless steel 316L has been used for the fabrication of rolls (sink, guiding and stabilizing). For bearings, Co-based super alloys have been adopted by the galvanizers. Other approaches, including rolls surface treatment with ceramic and WC coatings, have also been reported in the literature [18,19].

This study is dedicated to the corrosion of 316L stainless steel (SS) in the Zn-55%Al-1.6%Si coating alloy (AZ). Changes in IMCs phases and alloy chemistry were predicted with the help of FactSage, a thermodynamic software. A static immersion test was conducted to validate the thermodynamic predictions and also to study the IMCs interfacial layer morphology with immersion time. The galvanizing pot gear's (sink and guiding rolls, snouts) integrity has been a longstanding issue in the industry. Therefore, this study has been explicitly dedicated to the interaction of pot gears material (316L SS), with Al-Zn-Si coating alloy under industrial conditions (600 °C). Our aim is that the outcomes of this study shall facilitate the galvanizers to better understand the interaction of pot gears with molten Al-Zn-Si coating alloy and to plan a well-informed maintenance strategy.

2. Materials and Methods

2.1. Experimental Plan

To study the galvanizing pot gears degradation, static immersion tests were conducted. Stainless-steel (SS) 316L rods of 10 mm diameter were immersed in the Al-Zn-Si coating alloy. The 316L SS rods were obtained from a local supplier. Chemical compositions of the 316L SS rods and the Al-Zn-Si coating alloy are given in Table 1. The Al-Zn-Si coating alloy contains 0.40% Fe, which is the saturation limit of the alloy at 600 °C. This implies that the alloy is already saturated with Fe, hence there is limited drive for 316L SS rods dissolution in the alloy. Generally, 316L SS galvanizing pot gears (sink rolls, snout and guiding rolls) experience significant surface degradation with time during a continuous galvanizing coating process.

Table 1. Chemical compositions of the 316L SS and Al-Zn-Si coating alloy.

Elements	Fe	Cr	Ni	Mn	Si	Al	Zn	Minor
316L SS	70.9	17.9	9.4	0.9	0.6	0.1	-	Balance
AZ alloy	0.4	-	-	-	1.6	55	43	Balance

A schematic representation of the experimental set-up is shown in Figure 2. A resistant heated pot furnace was used in this study. Further, 2 kg of the Al-Zn-Si coating alloy was melted in the clay-bonded graphite crucible. K-type thermocouple was used to control melt temperature. Over the period of the entire experiment, 600 °C ± 1.5 °C temperature was maintained. The 316L SS rods were immersed in the molten Al-Zn-Si alloy and hanged with the SS wire, as shown in Figure 2. The 316L SS rods were removed from the alloy melt at different time intervals, starting from 24 h (1 day) to 168 h (7 days).

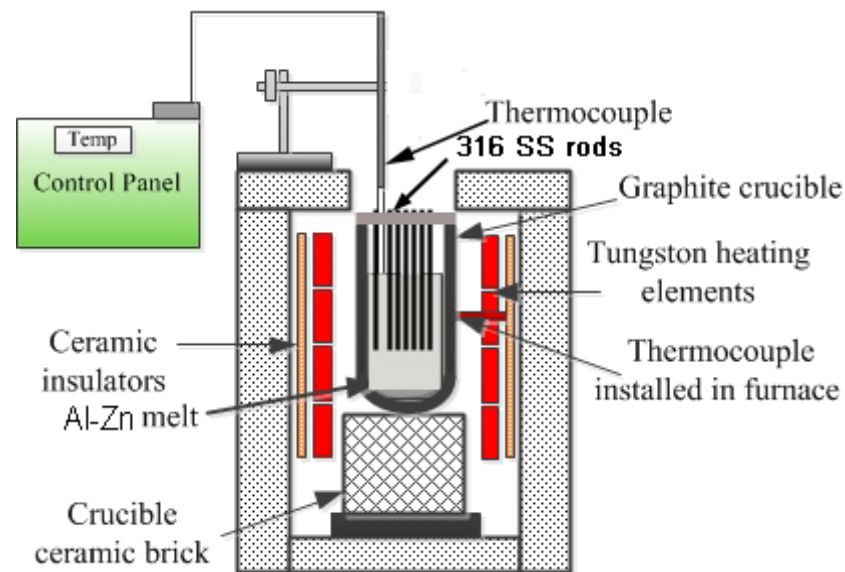


Figure 2. Schematic of the resistant pot furnace used in this study.

The 316L SS rods removed from the alloy melt after regular time intervals were allowed to cool naturally and were sectioned for further analysis. The dipped section of the rods was sectioned and hot mounted using a mounting press. The mounted samples are shown in Figure 3. As-received 316L SS and the statically immersed samples were prepared for the metallographic investigations.

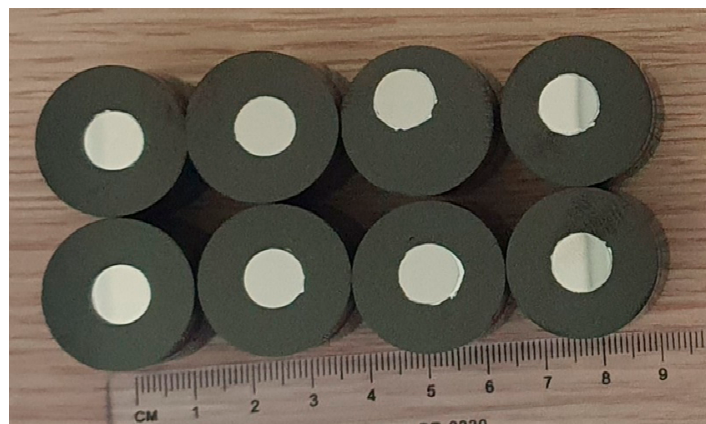


Figure 3. 316L SS samples immersed and mounted for further study.

The mounted samples were ground and polished following the Struers metallography procedure. Grinding was carried out using 220, 400, 800 and 1200 grit SiC emery papers at 300 rpm under a load of 25 N using water as a lubricant. Polishing was carried out using 9 μm and 3 μm diamond paste at 150 rpm under a load of 20 N. Final polishing was performed using alumina suspension at a load of 15 N and 150 rpm up to 5 to 10 min.

2.2. Characterization Techniques

An optical microscope (Leica DM 2500) and scanning electron microscope (FEI Nova, 200 FEGSEM (2007)) were used for the investigation of microstructural features of the IMCs layers formed during the dipping tests. The SEM was equipped with energy dispersive X-ray spectroscopy (EDS) for compositional analysis of the alloy layers. The microhardness of the 316L SS and IMCs layers was determined by the Vickers microhardness testing machine (VLS 3853, Shimadzu, Japan). The hardness testing was performed at the load of 0.05 kgf at a dwelling time of 5 s.

3. Thermodynamic Assessment of Al, Fe, Si, Cr, V and Si System

3.1. Thermodynamic Modeling

Thermochemical calculations using FactSage 7.2 software package were conducted to predict the equilibrium products and their compositions in the SS base metal, AZ coating and at the interface of the base metal and the coating at different processing temperatures. The FactSage pure compound database FactPS and FactSage solution databases FTstel and FTlite were used in this study. The NIST-JANAF thermochemical tables and NBS (National Bureau of Standards) tables of chemical thermodynamics were utilized to source the standard thermodynamic compilation data for the calculations in FactSage. The 'Equilib' module was used for the calculations of the concentrations of chemical species at the equilibrium state using the Gibbs free energy minimization approach [20,21]. The calculations were carried out considering the most stable phases at various processing circumstances that were found in the literature. The assumptions made for the calculations were as follows:

- The reactions are conducted at ambient condition (one atmospheric pressure) but at different temperatures, which implies that the gaseous species composition has no influence.
- Unit activity of the elements is considered in the standard state, and all the atoms/molecules interact freely to attain the lowest energy state.
- The calculations are conducted at equilibrium, assuming that the lowest energy state is obtained independent of the reaction kinetics.
- The reactions are conducted in a closed system.

Based on the common literature, the data were input in this current thermodynamic modeling. The list of the equilibrium reaction products predicted from the model are shown in Table 2.

Table 2. Thermodynamic stable phases (products) that were utilized for FactSage calculations.

Gas	Liquid	Solid	Solid	Solid	Solid
Zn	Zn	Zn_BCT	Mn_HCP	Al ₁₂ (Fe,Mn)	Al ₃ Fe
Mn	Cr	Zn_DIAMOND	Al_BCC	AlNi	AL8MN5D810/(Al,Si) ₁₂ Mn ₄ (Al,Fe,Mn) ₁₀
Al	Al	Cr_BCC	Al_HCP	Al ₃ Ni ₂	Al ₁₃ Fe ₄ (FeAl ₃)
Cr	Solid	Cr_HCP	Al_CBCC	Al ₅ Fe ₄	Al ₄ Mn
Fe	Fe_BCC	Cr_CUB	Al_CUB	Al ₂ Fe	FeSi
Ni	Fe_FCC	Cr_CBCC	Al ₈ Cr ₅	Al ₅ Fe ₄₁	(Fe, Mn) ₃ Si
Al ₂	Fe_HCP	Ni_HCP	FeZn ₄	Al ₅ Fe ₂₁	Fe ₅ Si ₃
Si	Fe_ORTHORHO	Ni_BCC	Al ₄ Mn	Al ₅ Fe ₂₁	Al ₆ Mn
Si ₂	Fe_TETRAGON	Ni_CUB	Cr ₃ Si	NiZn ₈	Al ₁₁ Mn ₄₁
Si ₃	Zn_HCP	Ni_FCC	Al ₁₁ Cr ₂	Ni ₂ Si	
	Zn_BCC	Mn_FCC	Ni ₅ Si ₂	CrZn ₁₃	

3.2. Equilibrium Products

The equilibrium products in the 316L stainless-steel base, AZ coating and at the reaction zone of the SS base metal and the AZ coating were modeled using the FactSage software application. The equilibrium product phases and their composition were studied at different temperatures, ranging from 200 to 700 °C (Figure 4). Figure 4a, shows the product phases of AZ coating at different temperatures. Below 350 °C, only Al_FCC, Zn_HCP and Si_DIAMOND phases were obtained. Above 350 °C, liquid starts to form at the expense of the solid phases. The initial liquid is rich with Zn and with an increase in temperature, Al, Si and Fe (from the dissociation of Al₁₄Fe₃Si₃) gradually diffused to the liquid. The formation of the liquid phase was completed at 550 °C.

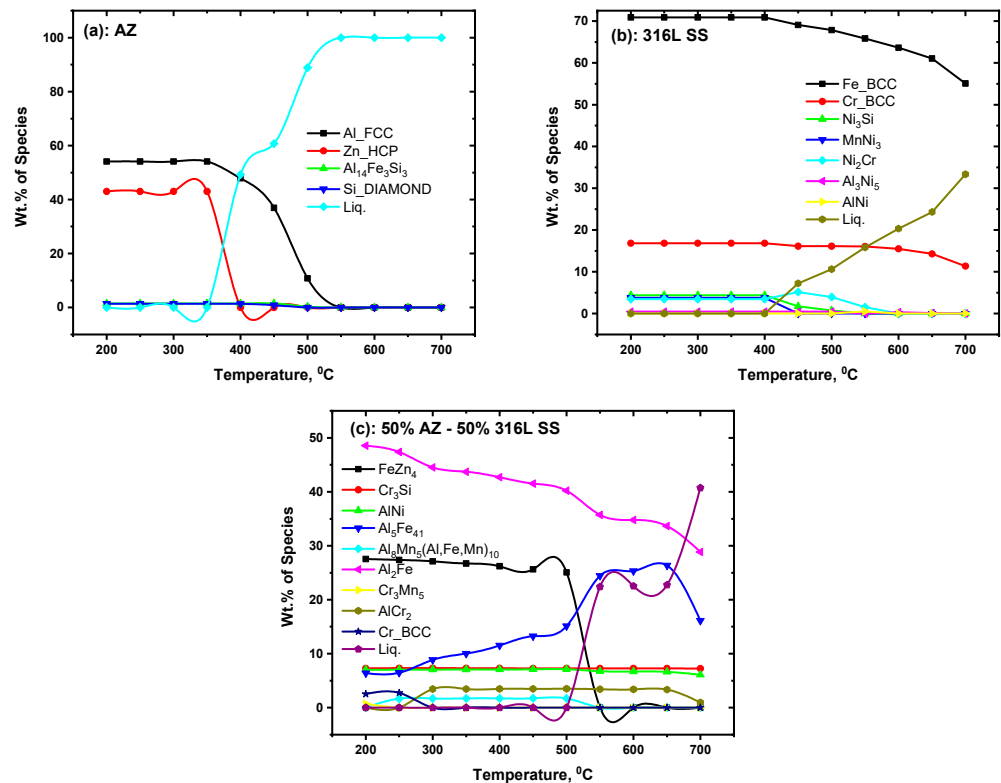


Figure 4. Equilibrium products and their compositions in the (a) AZ coating, (b) SS base metal and (c) at the interface of the base metal and the coating (optimized for 50% AZ and 50% SS) at different processing temperatures ranging from 200 to 700 °C.

Figure 4b, shows the product phases of 316L stainless-steel base metal at different temperatures. The solid phases present in the SS base metal at temperatures lower than 450 °C are Fe₂BCC, Cr₂BCC, Ni₃Cr, MnNi₃, Ni₂Cr, Al₃Ni₅ and AlNi. According to the FactSage modeling results, liquid starts to form at 450 °C and is increased with temperature. Maximum amount of 33.4% of liquid is obtained at 700 °C. Figure 4c shows the product phases in the reaction zone at different temperatures. The reaction zone was simulated in the calculation by setting the composition of the equal weightage of the base metal and the AZ coating composition. Interestingly, in the reaction zone, liquid starts to form at much higher temperature of 550 °C, at the expense of the FeZn₄ phase and Al₂Mn₅(Al,Fe,Mn)₁₀ or (Al,Si)₁₂Mn₄(Al,Fe,Mn)₁₀ phase. The fraction of the Al₂Fe phase and AlNi was gradually decreased with increasing temperature from 550 °C. However, the liquid amount was not increased until the process temperature was higher than 650 °C. It is also of note that the amount of solid Al₅Fe₄₁ was increased with increasing temperature till 650 °C; beyond 650 °C, the amount of Al₅Fe₄₁ was significantly decreased, yielding a higher amount of liquid.

The composition of the liquid phases 316L stainless-steel base, AZ coating and at the reaction zone of the SS base metal and the AZ coating was studied in detail. Figure 5a shows that the initial liquid phase in the AZ coating was rich with Zn and Fe. Above 450 °C, Al started to dissolve from the solid phase, which was completed at 550 °C. As seen in Figure 5b, the initial liquid phase in the stainless-steel base was mainly composed of Ni, Mn, Fe and Cr.

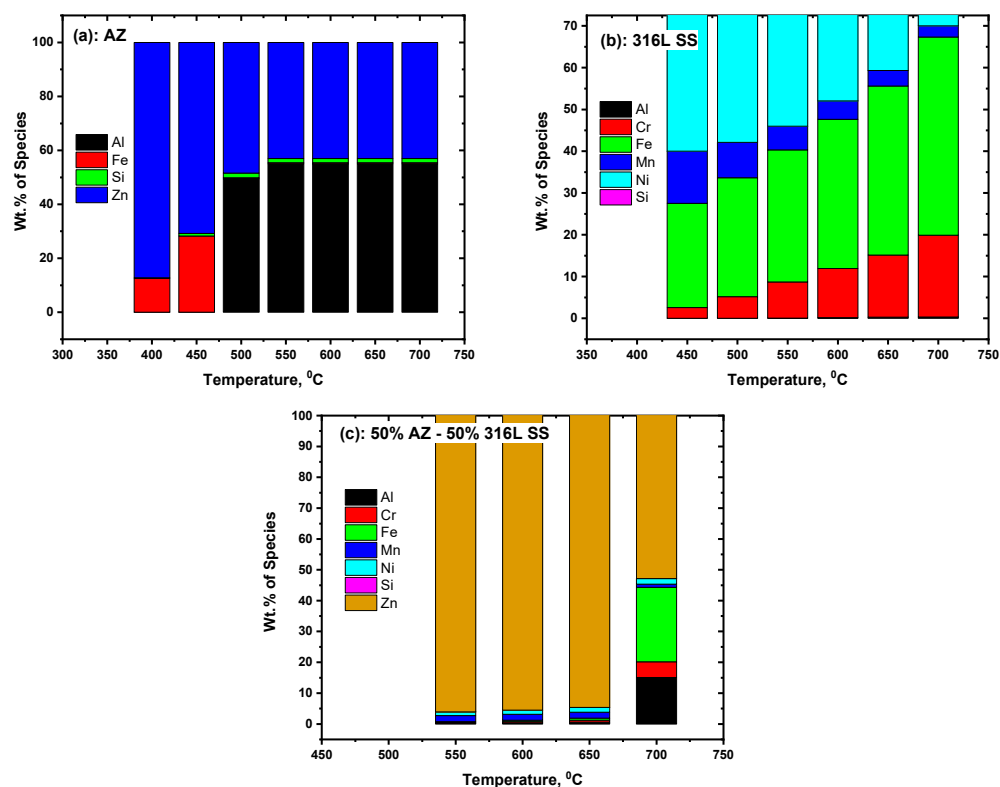


Figure 5. Equilibrium compositions of the liquid phase in the (a) AZ coating and (b) SS base metal (c) at the interface of the base metal and the coating (optimized for 50% AZ and 50% SS) at incremental processing temperatures to 700 °C.

The initial liquid was probably formed by the dissociation of Ni_3Si and MnNi_3 phases that reacted with solid iron to form the liquid. With increasing temperature, the content of Fe and Cr in the liquid was increased while the content of Ni and Mn was decreased. The increase in temperature promoted the dissolution of Fe and Cr from solid phase and the dissociation of Ni_2Cr phase. In the reaction zone, the initial liquid was found highly rich in Zn, which came from the AZ coating. The composition of the liquid was almost unchanged till the temperature was 650 °C. Above 650 °C, Fe, Al and Cr from the SS base started to dissolve to the liquid.

4. Results and Discussion

4.1. Microstructural Analysis of the Interface

Figure 6 shows an optical microscope (OM) image of the as-received 316L SS and the immersed samples in the AZ coating alloy at 600 °C from 1 day to 7 days.

The as-received 316L SS cross section mounted in epoxy is shown in Figure 6a. It is evident from Figure 6b–h that a severe reaction took place at the interface of the SS and AZ coating alloy during the static immersion at 600 °C. As a result, an interfacial intermetallic (IMC) layer developed over the entire 316L SS substrate. After 1 day of immersion, a single IMC layer was formed, as shown in Figure 6b. However, with extended immersion time (2–7 days), a second type of IMC layer was observed, see Figure 6c–h. This suggests that the initial reaction between 316L SS and AZ is significantly faster, as the IMC layer was observed even after 1 day of immersion. Moreover, the interfacial reactions evolved with extended immersion time to develop a second type of the IMC layer. Yet another key feature of the interfacial IMC layers is the development of a crack within the layers. This suggests that the 316L SS surface properties will deteriorate entirely with immersion time. Moreover, the cracked IMC layers will detach from the substrate and fall down in the coating pot. Such interlayer cracks have also been reported earlier [22]. Ultimately, this event shall also contribute to the bottom dross formation in the coating pot.

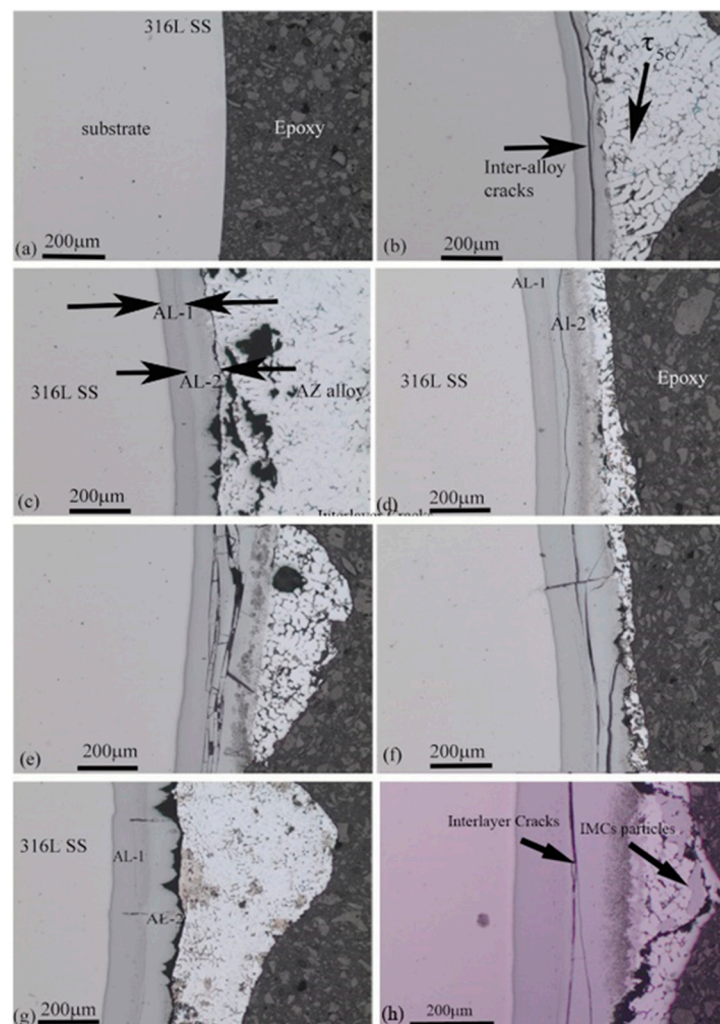


Figure 6. An optical microscopy (OM) image of AZ-alloy-immersed 316L SS samples (a) as received SS, (b) 1 day, (c) 2 days, (d) 3 days, (e) 4 days, (f) 5 days, (g) 6 days, (h) 7 days of immersion time at 600 °C.

The interfacial IMC layer, which developed adjacent to the SS substrate, is represented as IMC layer 1 (AL-1) and that formed between AL-1 and AZ coating overlay is represented as IMC layer 2 (AL-2). It is clear from Figure 4c–h that the surface morphology of both IMC layers is distinct and may possess different chemistry, as well as mechanical properties. At this stage, the type and crystallography of the interfacial IMC layers are not clear.

The SEM-SEI image of the 316L SS sample immersed for 7 days in the AZ coating alloy at 600 °C is shown in Figure 7. In addition to AL-1 and AL-2, the oxidation interface is also detected between the AL-2 and AZ coating overlay. This suggests 316L SS surface oxidation during immersion tests. Such oxidation is unavoidable during open-environment immersion tests, which has already been reported by previous researchers [5]. Special precautions, including conducting experiments in an ultra-high vacuum, coating steel surfaces with fluxes or masking tapes, could be beneficial in controlling the initial surface oxidation. However, from the hot-dip galvanizing perspective, the former measures are not relevant as the process is performed in an open environment. The AZ coating overlay microstructure has been reported earlier [9] and is shown in Figure 7. The microstructure includes a grey α -Al matrix with bright β -Zn at interdendritic regions. Si is also reportedly found in the interdendritic regions. Such coating alloys provide two levels of corrosion protection to the steel products, including first-level Al and second-level interfacial IMC layers.

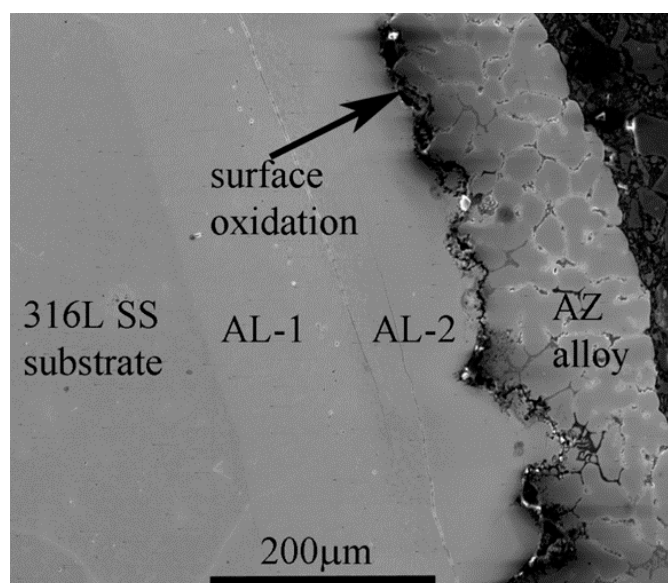


Figure 7. SEM-SEI image of SS sample after 7 days of immersion in the AZ alloy.

A close observation of the interfacial IMC layers reveals the presence of white submicron particles in the AL-1 interfacial IMC layer. These particles are even smaller in size and are located close to the 316L SS substrate compared to those found in the region adjacent to the AL-2. Moreover, these particles are uniformly distributed in the AL-1 matrix. The accurate type and crystallography of these white particles is not clear from this study. It is expected that these submicron particles are most likely Al-Cr and Al-Ni intermetallic particles. During immersion tests, 316L SS dissolved and released Fe, Ni and Cr in the AZ coating alloy. Considering the extremely low solubility of Ni and Cr in the AZ coating alloy, these elements will precipitate as intermetallic (Al-Cr), AlNi, as predicted during the thermodynamic analysis. The precipitation of Al-Cr intermetallic was reported by previous researchers [23]. Cracks in the inter-IMC layers are evident from Figure 7, suggesting AL-1 and AL-2 possess different thermal and mechanical properties. Such longitudinal cracks were also studied by previous researchers [24].

The interfacial IMC layers (AL-1 and AL-2) thicknesses change with immersion time, as shown in Figure 6. The AL-1 thickness increased from ~65 to 120 μm within 6 days of immersion time. Later, there was a marginal increase in thickness with one further day of immersion. Overall, there was a gradual increase in the AL-1 thickness with immersion time. The AL-2 formed after 1 day of immersion and grew up to ~150 μm within days. Similar to AL-1, there was also a gradual thickness increase until day 5 for AL-2. Later on, the AL-2 thickness became unstable, which is evident from Figure 8.

4.2. Compositional Analysis of the IMC Layers

Chemical composition of the 316L SS substrate and interfacial IMC layers was determined using EDS analysis. Although this technique is not precisely accurate, it gives qualitative elemental analysis for the phases. Figure 9 shows point analysis of the 316L SS substrate obtained by the EDS. The presence of ~18% Cr and ~10% Ni confirm the SS grade used in this study. This is a typical chemical composition of the 316L SS. The EDS analysis of the AL-1 is shown in Figure 10. This interfacial IMC layer contains 52.4% Al, 33.4% Fe, 6.2% Cr, 3.7% Ni, 2.7% Zn and 0.6% Si. This composition suggested that the AL-1 is Fe_2Al_5 , which was also reported by Liu et al. [12]. Small amounts of Cr and Ni dissolved from the SS substrate, accumulated in the AL-1 IMCs phase, forming Al-Cr and Al-Ni intermetallic particles. The AL-2 EDS analysis is shown in Figure 11. This interfacial IMC layer is formed between AL-1 and AZ coating overlay that contains comparatively smaller amounts of Fe. This IMC layer contains 56.3% Al, 27.8% Fe, 5.1% Cr, 4.2% Ni, 3.8% Si and 2.7% Zn. This IMC layer is recognized as FeAl_3 , also reported by previous researchers [8,25].

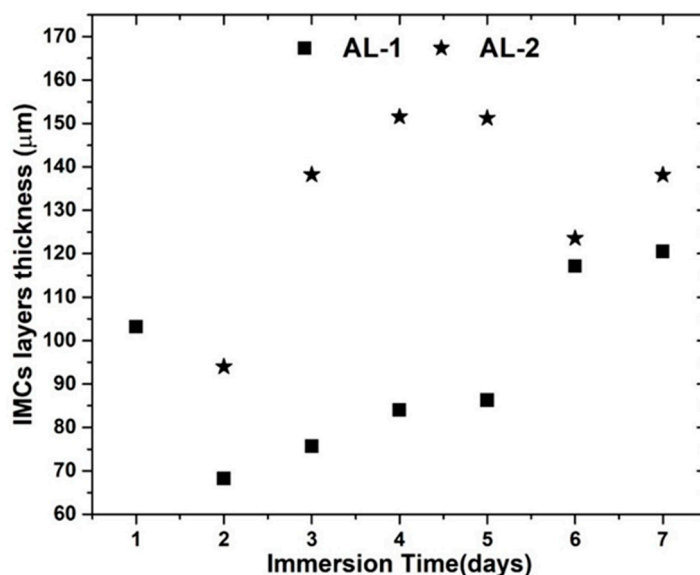


Figure 8. Change in the IMC layers (AL-1 and AL-2) thickness with immersion time (1 to 7 days) at 600 °C.

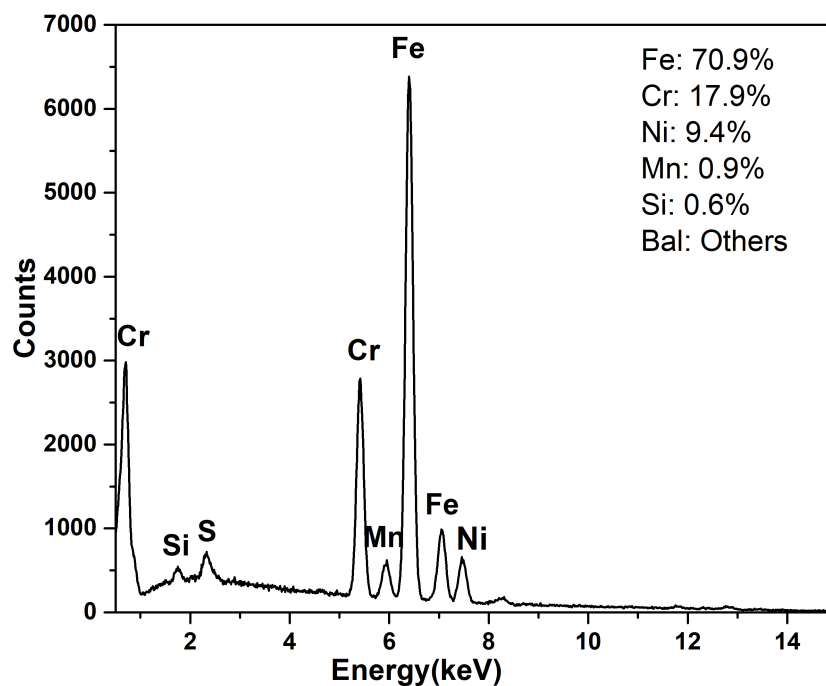


Figure 9. EDS analysis of the 316L SS substrate (See Figure 4).

An elemental line scan across the interfacial intermetallic layers was obtained through EDS analysis and is shown in Figure 12. An SEM-SEI image of the selected area of the SS, IMC layers and AZ coating alloy is shown in Figure 12a. The line scan started from the SS region, evident from the higher Fe, Cr and Ni contents until 38 µm, as shown in Figure 12b. Al increased significantly and Fe decreased in the interfacial intermetallic layers. This suggests Al mass transfer from the AZ coating alloy into the SS substrate. The IMC layers (AL-1 and AL-2) had a thickness of ~250 µm, as calculated from Figure 12b. These IMC layers developed within 7 days of immersion time at 600 °C. Al and Zn lines are clear in the AZ coating regions that started beyond 290 µm in the EDS line scan.

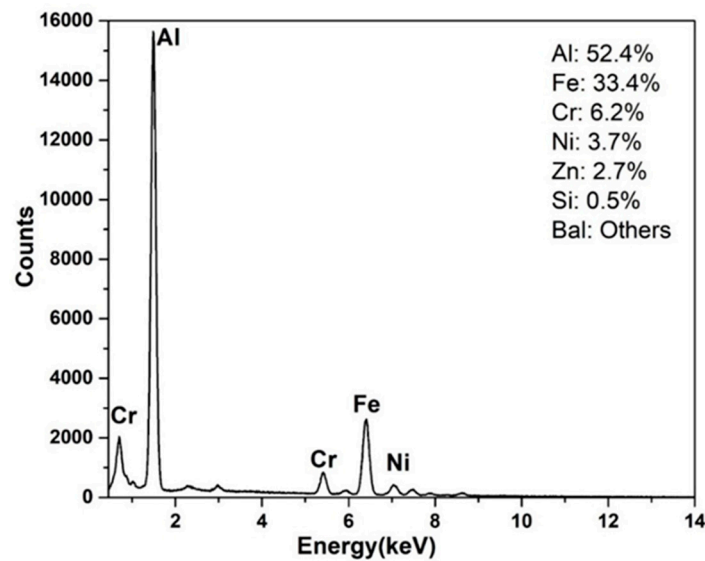


Figure 10. EDS analysis of the IMC layer (AL-1) (See Figure 4).

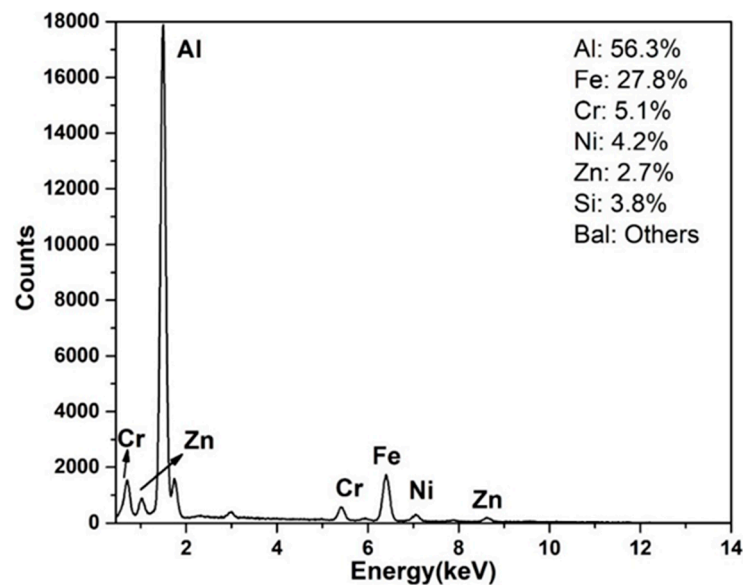


Figure 11. EDS analysis of the IMC layer (AL-2) (See Figure 4).

The corresponding Al, Fe, Zn, Cr, Ni and Si elemental maps were obtained using the EDS mapping method, shown in Figure 13. The Al-dominated regions include IMC layers and AZ coating alloy. The Fe contents were higher in the SS and gradually decreased in the IMC layers. Similarly, Cr and Ni contents dominated in the SS that diffused out into IMC layers; these are shown as discrete particles in Figure 13d,e. It is suggested that Cr will react with Al to form Al_7Cr and Al_4Cr discrete IMC particles, evident in Figure 13d. Such IMC particles precipitate during the solidification process due to extremely low Cr solubility in solid Al. Similarly, Ni that diffused out of the SS substrate also reacted with Al and other elements to form IMC particles that were predicted by the FactSage analysis, discussed in the earlier section. Figure 13e also suggests the precipitation of AlNi IMC particles in the interfacial IMC layers. Interestingly, relatively higher Cr contents are observed between the AL-1 and AL-2 interface, see Figure 13d.

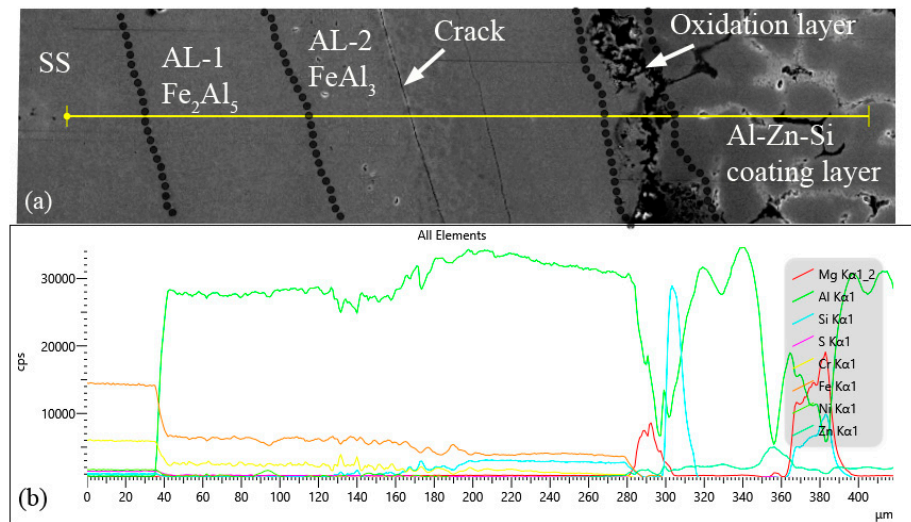


Figure 12. Elemental composition depth profiling from SS to AL-1, AL-2 and to AlZn alloy obtained using EDS technique. (a). SEM-SEI images, and (b). Elemental compositiona profile.

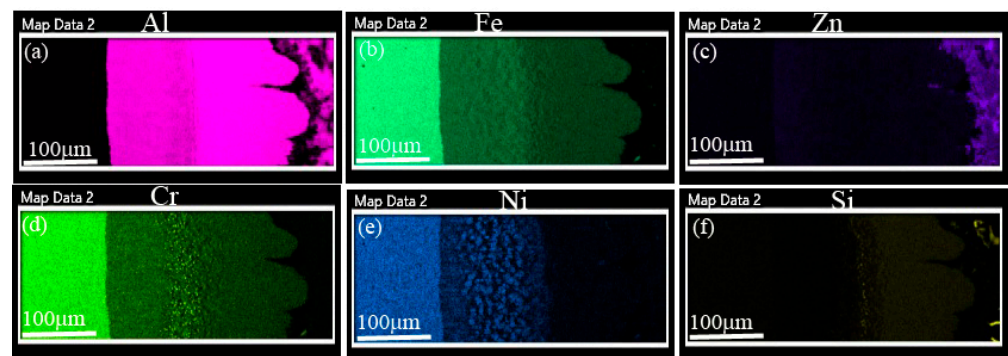


Figure 13. Elemental mapping of the SS, AL-1 and AL-2 obtained using EDS technique. (a). Al, (b). Fe, (c). Zn, (d). Cr, (e). Ni, (f). Si mapes.

5. Microhardness Analysis of SS, AL-1 and AL-2

The 316L stainless-steel substrate, AL-1A, AL-1B and AL-2 hardness are shown in Figure 14. The surface hardness of the SS substrate dramatically increased with immersion time. AL-1 dissected into AL-1A and AL-1B due to the presence of fine and discrete Al (Cr, Ni) IMC particles. The average Vicker's hardness (HV) of the SS substrate was 334 HV. However, hardness of the AL-1A IMC particle was 877 HV, which is ~2.62-times higher than the SS substrate. The hardness of the AL-1B IMC particle was 745 HV, which is lower than AL-1A. It is suggested that the presence of fine discrete Al-Cr/AlNi IMC particles increased AL-1A hardness. It is suggested that Cr and Ni mass transfer was limited, hence, their IMCs precipitated in the regions closer to the 316L SS substrate. This resulted in higher hardness in the AL-1 regions (AL-1A) adjacent to the SS substrate. The AL-2 hardness was 681 HV, which was lower than AL-1A and AL-1B. However, AL-2 hardness was still significantly higher compared to the SS substrate. AL-1 and AL-2 should exhibit different hardness due to individual crystallographic features. However, variation within the AL-1 is associated with the presence of embedded fine AlCr/AlNi IMC particles. The hardness findings are in agreement with previous work [13].

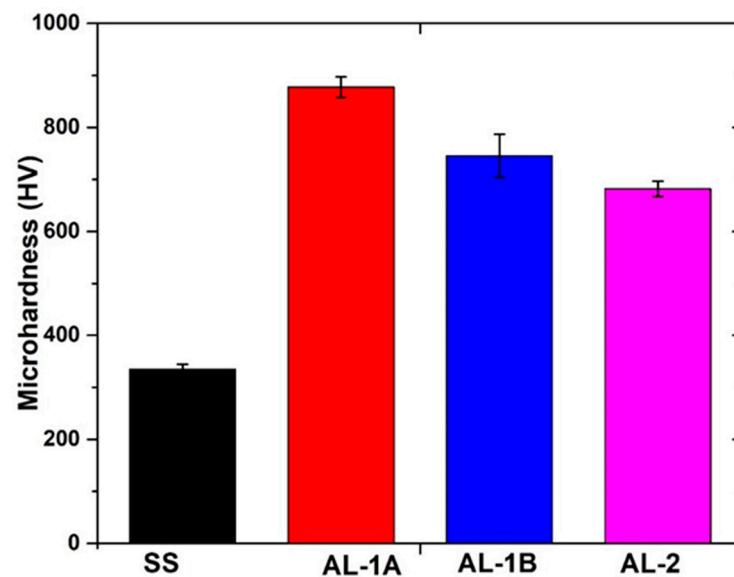


Figure 14. Vicker's microhardness of the SS and IMC layers.

6. IMC Layers Formation Mechanism

The intermetallic layers formation mechanism is proposed in this section and a schematic diagram is shown in Figure 15. The 316L SS pot gears, including sink rolls, are immersed in the molten Al-Zn-Si alloy at 600 °C. Generally, the immersion time varies from weeks to months, depending on the integrity of the pot gears and coated sheet quality. An equilibrium is attained between SS and Al-Zn-Si coating alloy with immersion time. Fundamentally, the SS reaction with molten Al-Zn-Si alloy is a solid–liquid reaction that exhibits extremely slow kinetics. Stainless-steel pot gears dissolution and mass transfer of Fe, Ni and Cr into a molten coating alloy is an inevitable process with immersion time. Simultaneously, Al, Zn and Si atoms shall migrate from bulk melt towards the SS surface. The migration of Fe, Ni and Cr atoms shall be opposite to that of Al, Zn and Si atoms. Considering the instant reaction of Al with Fe atoms, the FeAl_3 IMC layer is developed as soon as the SS surface is exposed to the Al-Zn-Si coating alloy. Such IMC layer thickness grows with immersion time. The second Fe-rich IMC phase (Fe_2Al_5) is developed with extended immersion time between the SS substrate and initially developed FeAl_3 IMC layer. It is suggested that Al atoms shall migrate from bulk melt through the FeAl_3 IMC layer and react with Fe to form an Fe_2Al_3 IMC layer adjacent to the SS substrate. It could be suggested that an equilibrium is established between SS/ Fe_2Al_5 / FeAl_3 couples. Moreover, interlayer cracks are developed due to different mechanical properties in the SS substrate, Fe_2Al_5 and FeAl_3 layers. Consequently, pot gears (sink rolls, snouts, etc.) surface properties are compromised with extended immersion time. The cracked FeAl_3 layer detached from certain regions of the sink rolls, hence, depressions are created on the surface, which stabilize and guide the steel sheet into and out of the coating pot. Therefore, steel sheets become unstable, which results in a poor coating quality.

Figure 15 illustrates the SS reaction with Al-Zn-Si coating alloy and formation of the IMCs layer. The Fe_2Al_5 IMC layer develops between the FeAl_3 and SS substrate, represented as a continuous dark layer. Between the Fe_2Al_3 and Al-Zn-Si coating alloy is FeAl_3 , which was represented as a grey layer. In addition to that, submicron white particles embedded in the Fe_2Al_5 layer are Al, Cr, Ni IMC particles that were predicted by the thermodynamic analysis.

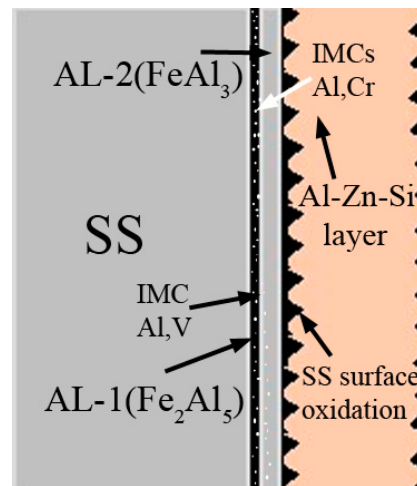


Figure 15. A schematic illustration of IMC layers formation during SS immersion in the Al-Zn-Si coating alloy.

7. Conclusions

This study investigated the intermetallic compound (IMC) interfacial layer formation between 316L stainless steel and an Al-Zn-Si coating alloy under industrial coating conditions. It can be concluded from this study that:

- The 316L SS reacts with the Al-Zn-Si coating alloy at 600 °C. As a result, two distinct IMC layers are developed between the SS substrate and AZ coating alloy.
- Iron diffusion from the SS substrate into AZ melt and Al mass transfer into a solid SS substrate are inevitable. The chemical reaction between Al and Fe is rapid, which forms Fe-based IMC layer at the interface.
- The interfacial layer is composed of two distinct intermetallic compounds (IMCs). The layer adjacent to the SS substrate is Fe_2Al_5 (AL-1) and that formed adjacent to the AZ coating alloy is FeAl_3 (AL-2). The EDS analysis confirms nature of the IMC layers. These findings are in agreement with the previous works.
- Cr and Ni diffused out from the SS substrate to form discrete $\text{Al}_7\text{Cr}/\text{Al}_4\text{Cr}$ and AlNi IMC particles. It is suggested that such IMC particles precipitate during the solidification process, once Cr and Ni solubility have decreased with temperature.
- The FactSage thermodynamic analysis also predicted the formation of AlCr and AlNi IMC particles, in addition to Fe_2Al_5 and FeAl_3 .
- The 316L SS surface hardness increased significantly during immersion in the AZ coating alloy at 600 °C. The AL-1 and AL-2 hardness was 877 HV and 681 HV, respectively.
- A longitudinal crack developed between the AL-1 and AL-2 IMC layers, which is one of the key findings of this study.

Author Contributions: Conceptualization, A.K. and A.S.A.; methodology, T.S.; software, M.M.H.; validation, A.K., M.M.H. and M.R.; formal analysis, A.K.; investigation, A.K.; resources, A.S.A.; data curation, W.H.; writing—original draft preparation, A.K.; writing—review and editing, W.H.; W.R.; T.S.; visualization, A.K.; supervision, A.K.; project administration, A.K. and A.S.A.; funding acquisition, A.K. and A.S.A. All authors have read and agreed to the published version of the manuscript.

Funding: This research has been funded by the Scientific Research Deanship at the University of Ha'il—Saudi Arabia (project number RG-20041) and The APC was funded by [RG-20041].

Institutional Review Board Statement: Not applicable.

Informed Consent Statement: Not applicable.

Data Availability Statement: Not applicable.

Acknowledgments: This research was funded by the Scientific Research Deanship at the University of Ha'il—Saudi Arabia (project number RG-20041).

Conflicts of Interest: The authors declare no conflict of interest.

References

1. Marder, A.R. The Metallurgy of zinc-coated steel. *Prog. Mater. Sci.* **2000**, *45*, 191–271. [CrossRef]
2. Setargew, N.; Hodges, J.; Parker, D. *Dross Intermetallic Formation and the Alloy Layer in 55%Al-Zn Coating Systems*; Steel Research Hub, University of Wollongong: Wollongong, Australia, 2015; pp. 1–30.
3. Borzillo, A.R.; Horton, J.B. Ferrous Metal Article Coated with an Aluminum Zinc Alloy. U.S. Patent 3,343,930, 26 September 1967.
4. Borzillo, A.R.; Horton, J.B. Method of Forming Improved Zinc-Aluminum Coating on Ferrous Surfaces. U.S. Patent 3,393,089, 16 July 1968.
5. Khaliq, A.; Parker, D.J.; Setargew, N.; Kondoh, K.; Qian, M. Dissolution Kinetics of Iron-Based Intermetallic Compounds (τ 5c IMCs) in a Commercial Steel Strip Metallic Alloy Coating Process. *Metall. Mater. Trans. B* **2021**, *52*, 41–50. [CrossRef]
6. Willis, D.J.; Setargew, N. *Bottom Dross Formation Mechanisms in Zinalume Coating Line Pots*; InterZAC: Seoul, Korea, 2002; pp. 1–17.
7. Williams, J.; Smith, R.; Neufeld, A.K. *An Investigative Study of Phase and Structure Formation in AM Coatings, Corrosion & Prevention*; Australasian Corrosion Association (ACA): Brisbane, Australia, 2013.
8. Khaliq, A.; Parker, D.J.; Setargew, N.; Qian, M. Fabrication of the τ 5c Intermetallic Compound Monoliths by a Novel Powder Metallurgy and Hot-Dipping Approach. *Metall. Mater. Trans. B* **2020**, *51*, 836–849. [CrossRef]
9. Chen, R.Y.; Yuen, D. Microstructure and crystallography of Zn-55Al-1.6Si coating spangle on steel. *Metall. Mater. Trans. A Phys. Metall. Mater. Sci.* **2012**, *43*, 4711–4723. [CrossRef]
10. Setargew, N.; Willis, D.J.; Thompson, D. *Detection of Dross Intermetallic Particles in 55%Al-Zn Melt Using LAIS*; InterZAC: Seoul, Korea, 2004; pp. 1–16.
11. Tang, N. *Dross Management in Continuous Galvanizing*; Cominco Ltd.: Mississauga, ON, Canada, 1999.
12. Liu, X.; Barbero, E.; Xu, J.; Burris, M.; Chang, K.M.; Sikka, V. Liquid metal corrosion of 316L, Fe₃Al, and FeCrSi in molten Zn-Al baths. *Metall. Mater. Trans. A* **2005**, *36*, 2049–2058. [CrossRef]
13. Khaliq, A.; Subhani, T.; Ali, H. Analysis of 316L Stainless Steel Interaction with Galvanizing Alloy Bath. *Microsc. Microanal.* **2020**, *26* (Suppl. 2), 2884–2886. [CrossRef]
14. Dybkov, V.I. Interaction of ¹⁸Cr-¹⁰Ni stainless steel with liquid aluminum. *J. Mater. Sci.* **1990**, *25*, 3615–3633. [CrossRef]
15. Loto, R.T.; Özcan, E. Corrosion Resistance Studies of Austenitic Stainless Steel Grades in Molten Zinc-Aluminum Alloy Galvanizing Bath. *J. Fail. Anal. Prev.* **2016**, *16*, 427–437. [CrossRef]
16. Zhang, K.; Battiston, L. Sliding wear of various materials in molten zinc Sliding wear of various materials in molten zinc. *Mater. Sci. Technol.* **2002**, *18*, 1551–1560. [CrossRef]
17. Yuan, B.; Liao, D.; Jiang, W.; Deng, H.; Li, G. Investigation on corrosion mechanism of stirring paddles of different iron-based materials in ZL101 aluminum melt. *J. Mater. Res. Technol.* **2021**, *13*, 1992–2005. [CrossRef]
18. Xu, J.; Bright, M.A.; Liu, X.; Barbero, E. Liquid Metal Corrosion of 316L Stainless Steel, 410 Stainless Steel, and 1015 Carbon Steel in a Molten Zinc Bath. *Metall. Mater. Trans. A* **2007**, *38*, 2727–2736. [CrossRef]
19. Zhang, K.; Tang, N.Y.; Goodwin, F.E.; Sexton, S. Goodwin, Scott Sexton, Reaction of 316L stainless steel with a galvanizing bath. *J. Mater. Sci.* **2007**, *42*, 9736–9745. [CrossRef]
20. Available online: www.factsage.com (accessed on 10 March 2022).
21. Bale, C.W.; Chartrand, P.; Deckerov, S.A.; Eriksson, G.; Hack, K.; Mahfoud, R.B.; Melançon, J.; Pelton, A.D.; Petersen, S. FactSage Thermochemical Software and Databases. *Calphad J.* **2002**, *62*, 189–228. [CrossRef]
22. Bellini, C.; Carlino, F. Intermetallic phase kinetic formation and thermal crack development in galvanized DCI. *Frat. Integrata Strutt.* **2019**, *48*, 740–747. [CrossRef]
23. Khaliq, A.; Ali, H.T.; Yusuf, M. Thermodynamic and kinetic analysis of CrB₂ and VB₂ formation in molten Al–Cr–V–B alloy. *Trans. Nonferrous Met. Soc. China* **2021**, *31*, 3162–3176. [CrossRef]
24. Rajhi, W.; Ayadi, B.; Khaliq, A.; Al-Ghamdi, A.; Ramadan, M.; Al-shammrei, S.; Boulila, A.; Aichouni, M. Constitutive behavior and fracture of intermetallic compound layer in bimetallic composite materials: Modeling and application to bimetal forming process. *Mater. Des.* **2021**, *212*, 110294. [CrossRef]
25. Kobayashi, S.; Yakou, T. Control of intermetallic compound layers at interface between steel and aluminum by diffusion-treatment. *Mater. Sci. Eng. A* **2002**, *338*, 44–53. [CrossRef]